

AD-A283 803



REPO		
1 AGENCY USE ONLY	2 REPORT DATE 1994	3 TYPE/DATES COVERED
4 TITLE AND SUBTITLE CORRELATION OF FATIGUE CRACK GROWTH RATE AT DIFFERENT STRESS RATIOS FOR QUENCHED AND TEMPERED STEELS AND OTHER ALLOYS		5 FUNDING NUMBERS
6 AUTHOR I M ROBERTSON		8 PERFORMING ORG. REPORT NO
7 FORMING ORG NAMES/ADDRESSES DEFENCE SCIENCE AND TECHNOLOGY ORGANIZATION, MATERIALS RESEARCH LABORATORY, PO BOX 50, ASCOT VALE VICTORIA 3032 AUSTRALIA		
09 SPONSORING/MONITORING AGENCY NAMES AND ADDRESSES		
11 SUPPLEMENTARY NOTES		
12 DISTRIBUTION/AVAILABILITY STATEMENT DISTRIBUTION STATEMENT A		128 DISTRIBUTION CODE
13. ABSTRACT (MAX 200 WORDS): MEASUREMENTS OF THE EFFECT OF STRESS RATIO ON THE CONSTANT AMPLITUDE FATIGUE CRACK GROWTH RATES IN FOUR QUENCHED AND TEMPERED STEELS IN THE PARIS REGIME ARE REPORTED. THIS DATA AND PUBLISHED DATA FOR OTHER ALLOYS (INCLUDING LOWER STRENGTH STEELS AND NON-FERROUS ALLOYS) ARE EVALUATED, AND A CORRELATION FUNCTION SUITABLE FOR PRACTICAL FATIGUE LIFE CALCULATIONS IS DERIVED. IN ADDITION TO STRESS INTENSITY FACTOR RANGE AND STRESS RATIO, OTHER SIGNIFICANT PARAMETERS ARE THE YIELD STRESS OF THE MATERIAL AND ITS THICKNESS. FOR THE FOUR STEELS ON WHICH NEW MEASUREMENTS WERE MADE, THE DEGREE OF DEPENDENCE OF THE CRACK GROWTH RATE ON STRESS RATIO MAY BE RELATED TO SENSITIVITY TO ENVIRONMENTAL CONDITIONS.		
14 SUBJECT TERMS		15 NUMBER OF PAGES 12
		16 PRICE CODE
17 SECURITY CLASS. REPORT UNCLASSIFIED	18 SEC CLASS PAGE UNCLASSIFIED	19 SEC CLASS ABST. UNCLASS
20 LIMITATION OF ABSTRACT		



1398 94-27270

This document has been approved for public release and sale; its distribution is unlimited.

94 8 25 047

**Best
Available
Copy**

CORRELATION OF FATIGUE CRACK GROWTH RATE AT DIFFERENT STRESS RATIOS FOR QUENCHED AND TEMPERED STEELS AND OTHER ALLOYS

I. M. ROBERTSON

Department of Defence, DSTO - Materials Research Laboratory, PO Box 50, Ascot Vale, Vic. 3032, Australia

Abstract—Measurements of the effect of stress ratio on the constant amplitude fatigue crack growth rates in four quenched and tempered steels in the Paris regime are reported. This data and published data for other alloys (including lower strength steels and non-ferrous alloys) are evaluated, and a correlation function suitable for practical fatigue life calculations is derived. In addition to stress intensity factor range and stress ratio, other significant parameters are the yield stress of the material and its thickness. For the four steels on which new measurements were made, the degree of dependence of the crack growth rate on stress ratio may be related to sensitivity to environmental conditions.

NOMENCLATURE

- a = crack length
- C, D = Paris coefficients
- ΔK = full stress intensity factor range
- ΔK_{eff} = effective part of ΔK
- ΔK_{tens} = tensile part of ΔK
- n = Paris exponent
- N = number of fatigue cycles
- P_{max} = maximum load in fatigue cycle
- R = stress ratio
- t = thickness
- $U(R)$ = crack closure function
- $V(R)$ = crack growth rate correlation function
- σ_y = yield stress

INTRODUCTION

The present work is concerned with fatigue crack growth rates in the Paris regime (or Stage II crack growth region). To a first approximation, fatigue crack growth in the Paris regime in metallic materials under constant amplitude loading is described by the Paris-Erdogan relation:

$$\frac{da}{dN} = C(\Delta K)^n \quad (1)$$

There have been a large number of studies resulting in the modification of Eq. (1) to incorporate the second order effect of mean stress (or stress ratio) and other variables. Some of the equations that have been proposed were tabulated by Chand and Garg [1].

In the present work the formulation presented by Elber [2] is followed. The crack growth rate

is regarded as a function of ΔK and the stress ratio, R :

$$\frac{da}{dN} = \frac{da}{dN}(\Delta K, R) = \frac{da}{dN}(\Delta K_{\text{eff}}) = \frac{da}{dN}(U\Delta K) \quad (2)$$

where U is regarded as a function of R only. Although Elber associated $U(R)$ with the portion of ΔK for which the crack is actually open, in the present work the function is treated simply as an empirical function for the correlation of fatigue crack growth rates in a material under different stress ratios. As discussed by Schijve [3], this type of $U(R)$ can be obtained from experimental data by measuring the relative displacement of $\log(da/dN)$ versus $\log(\Delta K)$ curves for different stress ratios.

The Paris-Erdogan relation is rewritten in the following way to incorporate stress ratio:

$$\frac{da}{dN} = D(\Delta K_{\text{eff}})^n = D[U(R)\Delta K]^n = C(R)(\Delta K)^n \quad (3)$$

The growth rates under different stress ratios at the same ΔK are then:

$$\begin{aligned} \frac{da}{dN}(\Delta K_1, R_1) &= D[U(R_1)\Delta K_1]^n \\ &= [U(R_1)/U(R_0)]^n \frac{da}{dN}(\Delta K_1, R_0) \end{aligned} \quad (4)$$

For equal growth rates at different stress ratios the stress intensity factor ranges required are given by:

$$\Delta K_0 = \Delta K_1 [U(R_1)/U(R_0)] \quad (5)$$

It should be noted that these equations apply only within the Paris regime and cannot be used for the threshold region or the high crack growth rate region (Stages I and III), where the effect of stress ratio is more pronounced.

Several different forms have been proposed for the function $U(R)$. Some of them are as follows:

(a) A basic correction which converts the full stress intensity factor range, ΔK , into the tensile part of the range, ΔK_{tens} . This will be referred to as the "basic correction", and is commonly the only correction for stress ratio effects that is applied in fatigue life calculations for structures containing residual stresses and other sources of mean stress.

$$\begin{aligned} U &= 1 && \text{for } R > 0 \\ &= 1/(1-R) && \text{for } R < 0 \end{aligned} \quad (6)$$

(b) Elber's formula (2):

$$U = 0.5 + 0.4R \quad \text{for } -0.1 < R < 0.7 \quad (7)$$

(c) Schijve's formula (Finney and Deirmendjian [4]) for aluminium alloys in the range $-1 < R < 0.7$

$$U = (0.55 - 0.2R - 0.25R^2 - 0.1R^3)/(1-R) \quad (8)$$

and similar polynomial expressions given in Refs [3] and [5].

(d) The formula of Kurihara *et al.* [6] for pressure vessel steels:

$$\begin{aligned} U &= 1 && \text{for } 0.5 < R < 0.8 \\ &= 1/(1.5 - R) && \text{for } -5 < R < 0.5 \end{aligned} \quad (9)$$

(e) The formula of Eason *et al.* [7] for ferritic steels in the range $0 < R < 0.9$

$$U = 1/(2.88 - R) \quad (10)$$

If the da/dN versus ΔK curve is known for a single stress ratio, R_0 , for the material in question (usually $R_0 = 0$), the steady state growth rate under any loading ΔK_1 , R_1 can be calculated from Eq. (4). This of course requires knowledge of $U(R_1)/U(R_0)$. Conversely, the value of $U(R_1)/U(R_0)$ can be obtained from fatigue crack growth rate curves for $R = R_1$ and $R = R_0$. It is not possible to obtain absolute values of $U(R)$ in this way, but neither is it necessary to have absolute values of $U(R)$ in order to calculate growth rates for stress ratios other than those for which data are available. All that is necessary is the ratio $U(R_1)/U(R_0)$.

We could use the function:

$$V(R) = U(R)/U(0) \quad (11)$$

as an empirical fatigue crack growth rate correlation function. However, it is more instructive to incorporate the basic correction (Eq. (6)) from the outset. This results in a correlation function identified here as $V'(R)$. It is derived as follows.

Equations (1)–(5) are modified by replacing ΔK with ΔK_{tens} (including new values of the material constants C and D) and the functions $U(R)$ and $C(R)$ are replaced respectively by the functions:

$$\begin{aligned} U'(R) &= U(R) && \text{for } R > 0 \\ &= (1 - R)U(R) && \text{for } R < 0 \end{aligned} \quad (12)$$

$$\begin{aligned} C'(R) &= C(R) && \text{for } R > 0 \\ &= (1 - R)C(R) && \text{for } R < 0 \end{aligned} \quad (13)$$

The empirical fatigue crack growth rate correlation function to be used here is then:

$$\begin{aligned} V'(R) &= U'(R)/U'(0) \\ &= V(R) && \text{for } R > 0 \\ &= (1 - R)V(R) && \text{for } R < 0 \end{aligned} \quad (14)$$

From Eq. (5), the crack growth rate at stress ratio R would equal that at $R = 0$ when the tensile component of the stress intensity factor range is:

$$\Delta K_{\text{tens}, R} = \Delta K_{\text{tens}, 0} / V'(R) \quad (15)$$

where $\Delta K_{\text{tens}, 0}$ is the tensile component of the SIF range at $R = 0$ (equal to ΔK). From Eq. (4) the growth rates at constant ΔK_{tens} are:

$$\frac{da}{dN}(\Delta K_{\text{tens}, R}) = \frac{da}{dN}(\Delta K_{\text{tens}, 0}) [V'(R)]^n \quad (16)$$

Figure 1 shows the function $V'(R)$ derived from Eqs (7)–(10), (12) and (14). Although the $U(R)$ functions differ quite significantly, the values of the corresponding $V'(R)$ functions are similar because of the normalisation to the value $U(0)$.

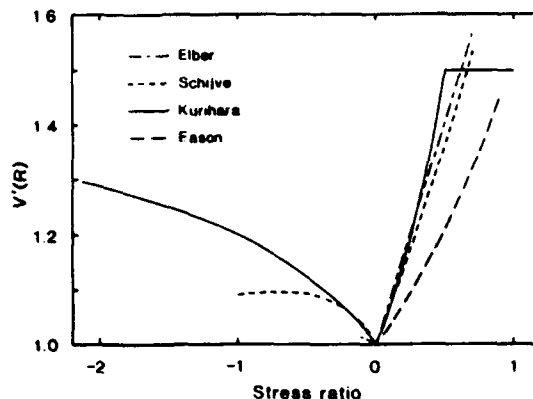


Fig. 1. Values of the crack growth rate correlation function $V'(R)$ derived from Eqs (7) to (10) for the closure function $U(R)$.

One of the goals of the present work was to decide why different materials or testing conditions give rise to different $V'(R)$ correlation functions. Four quenched and tempered steels were tested over a range of stress ratios between -2 and $+0.7$ to examine the effect of yield strength on the correlation function $V'(R)$. Published fatigue crack growth rate curves for other alloys were also re-examined and evaluated in terms of $V'(R)$.

MATERIALS AND METHODS

The compositions and tensile properties of the steel plates from which specimens were machined are listed in Table 1. All are high toughness, quenched and tempered steels used for submarine hull and other applications. The strength depends on the composition and the temperature of the tempering treatment applied to the steels after quenching. Centre-cracked fatigue specimens with a width, W , of 100 mm and thickness, B , of 12.5 mm were machined, and stress relieved at 600°C before grinding to final dimensions. Fatigue testing was carried out in laboratory air (about 20°C and 50% RH) under sinusoidal loading at a frequency of 3–5 Hz.

For each specimen the stress ratio was increased in a stepwise manner (minimising transient effects as described by Robertson [8]) so that the cracks extended by about 4 mm for each step of constant amplitude loading but the growth rate remained approximately 10^{-7} m/cycle. The loads that were applied are listed in Table 2. A single specimen of each steel was tested except for Q1N, which was used to confirm the reproducibility of the result [8]. Fatigue crack growth was

Table 1. Composition (%wt) and tensile properties of the four steels

Steel	%C	%Si	%Mn	%P	%S	%Ni	%Cr	%Mo	%Cu	%V
Q1N	0.16	0.25	0.31	0.010	0.008	2.71	1.42	0.41	0.10	0.01
	Proof stress: 570 MPa			UTS: 663 MPa						
Q2N	0.15	0.35	0.31	0.010	0.003	3.20	1.53	0.45	0.08	0.01
	Proof stress: 707 MPa			UTS: 823 MPa						
BIS	0.14	0.27	0.98	0.010	0.001	1.30	0.52	0.37	0.21	0.02
	Proof stress: 700 MPa			UTS: 770 MPa						
HY130	0.10	0.32	0.79	0.006	0.003	4.90	0.54	0.49	0.05	0.07
	Proof stress: 958 MPa			UTS: 1004 MPa						

Table 2. Sequence of loads applied to specimens (P_{max} in kN)

Q1N	R	-2.03	-1.04	-0.51	0.01	0.29		0.60	
	P_{max}	109.0	108.0	109.0	108.5	125.0		196.0	
Q2N	R			-0.48	0.01	0.20	0.41	0.60	0.71
	P_{max}			116.5	110.0	107.5	110.0	144.0	148.5
BIS	R			-0.49	0.01	0.20	0.40	0.61	0.70
	P_{max}			125.0	119.0	121.5	127.0	167.5	166.5
HY	R	-1.98	-1.01	-0.49	0.03	0.28		0.51	0.71
	P_{max}	122.5	108.5	98.0	94.5	103.0		127.0	159.5

monitored using a travelling microscope, and growth rates calculated using the seven point incremental polynomial method.

RESULTS

Quenched and tempered steels

Results for HY130 from the present work are shown in Fig. 2, where the full range of stress intensity factor has been plotted (to avoid overlapping curves). Results for Q1N were published previously (Fig. 3 of Ref. [8]). The remaining steels, Q2N and BIS812EMA, gave results similar to Q1N and HY130 except that testing was restricted to stress ratios between -0.5 and $+0.7$.

The values of the function $V'(R) = U'(R)/U'(0)$ for the different steels are compared in Fig. 3. Some additional data points extracted from the relative displacement of the crack growth rate curves of Jones [9] are also included (for Q1N and HY130 in laboratory air at $R = 0.5$ and a growth rate of 10^{-7} m/cycle). The sensitivity of the crack growth rate to stress ratio appears to increase with the yield strength of the steel at positive R , but the opposite trend applies for negative R .

The data points shown in Fig. 3 are approximated by the equations:

$$\text{Q1N} \quad R > 0: \quad V'(R) = 1 + 0.16R \quad (17)$$

$$\text{BIS} \quad R > 0: \quad V'(R) = 1 + 0.34R \quad (18)$$

$$\text{Q2N} \quad R > 0: \quad V'(R) = 1 + 0.36R \quad (19)$$

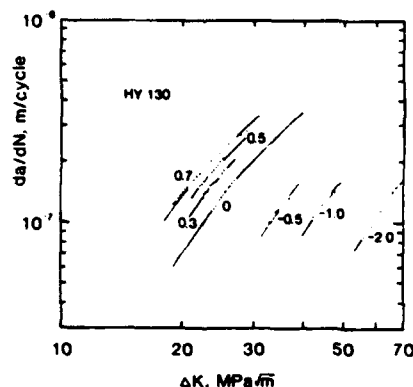


Fig. 2. Fatigue crack growth rate curves for HY130 steel in air for the stress ratios, R , of -2 , -1 , -0.5 , 0 , 0.3 , 0.5 , and 0.7 .

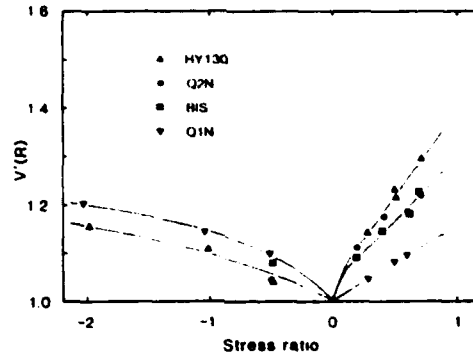


Fig. 3. Values of the crack growth rate correlation function $V'(R)$ for the steels Q1N, Q2N, BIS812EMA and HY130 from the present work (filled symbols) and from Jones [9] (open symbols at $R = 0.5$).

$$\text{HY130} \quad R > 0: \quad V'(R) = 1 + 0.44R \quad (20)$$

$$\text{All} \quad R < 0: \quad \begin{cases} V'(R) = 1.25(1 - R)/(1.25 - R) & (21) \\ V'(R) = 1 + \log(1 - R)/2.7 & (22) \end{cases}$$

Additional values of $V'(R)$ derived from published crack growth rate curves [6,10–13] for quenched and tempered steels are shown in Fig. 4. There are two sets of results for Q1N steel (both calculated from the relative displacement of growth rate curves at 10^{-8} m/cycle). Although James and Knott [10] found very little influence of R on the growth rate of long, through cracks in Q1N for R between 0.2 and 0.7 (similar to results for Q1N in Fig. 3), Cowling and Knott [11] found much greater sensitivity to R for short, semi-elliptical cracks in Q1N (even greater sensitivity than for HY130 in Fig. 3). As James and Knott, and Cowling and Knott did not report results for zero R , an extrapolation has been used to position the data point at $R = 0.2$ in each case. For example, the data of Cowling and Knott allow the values $V(0.35)/V(0.2)$, $V(0.5)/V(0.2)$ and $V(0.7)/V(0.2)$ to be determined, and extrapolated to obtain $V(0)/V(0.2)$. The reciprocal of this is $V'(0.2)$ and the other values plotted are given by $V'(R) = V'(0.2)[V(R)/V(0.2)]$.

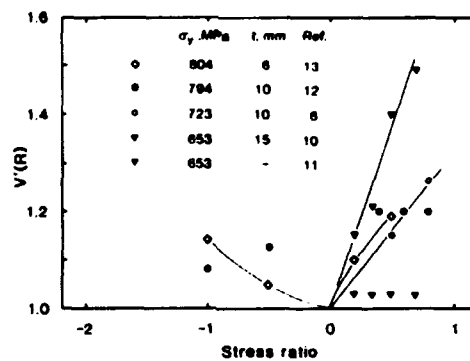


Fig. 4. Values of the correlation function $V'(R)$ derived from published fatigue crack growth rate curves for quenched and tempered steels. Values were obtained at growth rates between 10^{-8} and 10^{-7} m/cycle.

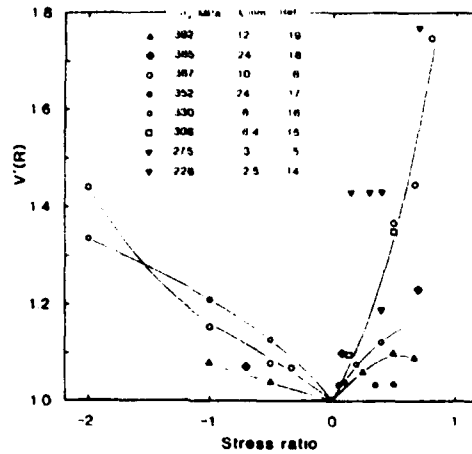


Fig. 5. As for Fig. 4 but for steels with yield stresses between 200 and 400 MPa.

Other steels

Except for the quenched and tempered steels considered above (with yield strengths ranging from about 550 to 1000 MPa), relevant data for steels appear to be available only for yield strengths between 200 and 400 MPa. The values of the correlation function $V'(R)$ derived from published crack growth rate curves [5,6,14–19] for these steels are shown in Fig. 5.

There is a considerable amount of scatter, as might be expected with data derived from a wide range of sources. However, trends are still apparent. For positive stress ratios, $V'(R)$ increases most rapidly with increasing R for lower strength steels tested at lower thickness. This can be attributed to larger plastic zone size relative to the thickness of the specimen, cracking under more-nearly plane stress conditions, and a greater degree of slant fracture (see Schijve [3], McEvily [20] for discussion of increased crack closure under plane stress conditions). This is the opposite trend to that observed for the quenched and tempered steels, where essentially plane strain conditions prevail and the fracture faces are nearly flat.

For negative stress ratios there are fewer data but it appears that steels of higher strength are less sensitive to R (as for the quenched and tempered steels).

Austenitic stainless steel, aluminium and titanium alloys

Figure 6 shows values of $V'(R)$ derived from published $U(R)$ functions for aluminium and titanium alloys [3], and from crack growth rate curves for an aluminium alloy [21] and type 304 stainless steel [15,22]. Most of the data are for positive R and show a strong dependence of crack growth rate on stress ratio for $R > 0$. As for the low strength steels considered above, this can be attributed to the large degree of crack closure and slant fracture due to the low thickness at which most of the alloys were tested.

DISCUSSION

Examination of Figs 3 and 5 suggested that yield strength and specimen thickness influence the values of the correlation function. Figure 7 shows the effect of yield stress for both groups of steels considered above. For most of the steels, $V'(R)$ increases approximately linearly as R increases or decreases from zero. Therefore, stress ratios of +0.5 and -0.5 have been selected to represent

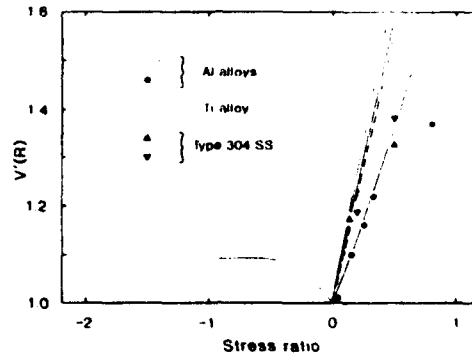


Fig. 6. As for Fig. 4 but for aluminium alloys [3,21], type 304 stainless steel [15,22] and a titanium alloy [3].

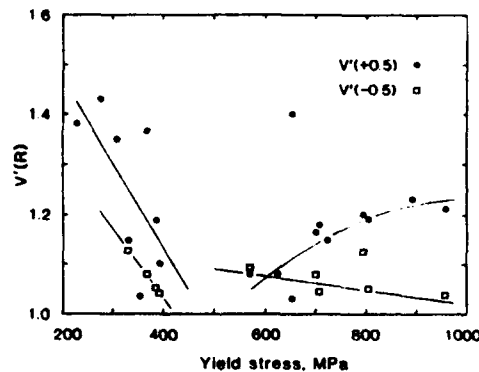


Fig. 7. Values of $V'(0.5)$ and $V'(-0.5)$ plotted against yield strength for the steels shown in Figs 3, 4 and 5.

positive and negative R respectively in Fig. 7. In some cases it was necessary to interpolate (linearly) between data points to obtain the $V'(R)$ value at $R = 0.5$ or -0.5 .

There is a large amount of scatter, especially for the lower strength steels. Some of this can be attributed to the fact that ΔK_{tens} , R and σ_y (or thickness) are not sufficient to characterize the material and crack growth conditions. However, a large part of the scatter probably arises from inaccuracies in the experimental determination of growth rates at different R , and in extracting the $V'(R)$ values from published crack growth rate curves. For the quenched and tempered steels there are two anomalous data points. The high value of $V'(0.5)$ for semi-elliptical cracks in Q1N steel [11] has been discussed above. The high value of $V'(-0.5)$ for a steel with a yield stress of 794 MPa [12] can be attributed to experimental scatter, as the corresponding $V'(-1)$ value is lower (Fig. 4).

For negative R the effect of yield strength on $V'(R)$ is weak, but $V'(R)$ is slightly higher for the lower strength steels. Specimen thickness does not appear to be a significant influence. A possible mechanism for the yield stress dependence is the crushing together of asperities on the fracture faces during the compressive part of the fatigue cycle. Linear regression relations for the data are as follows:

$$\text{Quenched and tempered: } V'(-0.5) = 1.15 - 0.11 \times 10^{-3} (\sigma_y/\text{MPa}) \quad (23)$$

(6 points, $r = -0.41$)

$$\text{Q and T (excluding [12]): } V'(-0.5) = 1.16 - 0.14 \times 10^{-3} (\sigma_y/\text{MPa}) \quad (24)$$

(5 points, $r = -0.82$)

$$\text{Lower strength steels: } V'(-0.5) = 1.59 - 1.4 \times 10^{-3} (\sigma_y/\text{MPa}) \quad (25)$$

(4 points, $r = -1.00$)

$$\text{Combined data (not [12]): } V'(-0.5) = 1.10 - 0.06 \times 10^{-3} (\sigma_y/\text{MPa}) \quad (26)$$

(9 points, $r = -0.48$)

For positive stress ratios, the quenched and tempered steels and the lower strength steels behave differently, but the effect of yield stress is much stronger than for negative R for both groups of steels. Thickness also appears to be significant, but only for the lower strength steels. Table 3 shows the results of linear regression analyses for $V'(0.5)$ against σ_y , t , $\sigma_y^2 t$ and $(1000 \text{ MPa} - \sigma_y)^2$. The parameter $\sigma_y^2 t$ was selected because the ratio of specimen thickness to crack-tip plastic zone size is proportional to

$$t/(K_{\max}/\sigma_y)^2 = \sigma_y^2 t/K_{\max} \quad (27)$$

and K_{\max} is already determined by ΔK and R . The anomalous data point for semi-elliptical cracks in Q1N [11] has been excluded.

It is recognized that crack closure at positive stress intensity is more prevalent under plane stress conditions than under plane strain [3,17,19,20,23], and that closure is largely irrelevant during the initial stages of fatigue cracking of a structure. On this basis we would expect that $V'(R)$ for positive R would decrease towards unity as the thickness or yield strength of the material increased. This is the trend observed for the lower strength steels in Fig. 7 and Table 3 (and suggests that crack closure is the mechanism for the dependence of crack growth rate on stress ratio in these steels).

However, the quenched and tempered steels do not behave in this way (either in the general trend of $V'(R)$ with yield stress, or in the specific case of semi-elliptical cracks in Q1N [11] where strong R dependence was observed). A possible explanation for the greater dependence of crack growth rate on stress ratio for the higher strength steels lies in their greater sensitivity to environment (rather than yield strength *per se*). The steels Q1N and HY130 were examined by Jones [9] in dry air, laboratory air and sea water. The steels HY80 and HY130 (HY80 is almost identical to Q1N) were examined by Kwun and Fine [24] in laboratory air and dry argon. These investigations showed that the two steels have similar crack growth rates in dry air or dry argon, but

Table 3. Linear regression equations for $V'(0.5)$ for steels. Yield stress, σ_y , in MPa, thickness, t , in mm

Steel group	No. of points	$V'(0.5)$	Regression coefficient
Q and T	10	$1.23 - 0.99 \times 10^{-6} (1000 - \sigma_y)^2$	-0.87
		$0.81 + 0.46 \times 10^{-3} (\sigma_y)$	+0.83
		$1.06 + 0.014 \times 10^{-6} (\sigma_y^2 t)$	+0.51
		$1.30 - 0.013 (t)$	-0.46
Lower σ_y	8	$1.81 - 1.7 \times 10^{-3} (\sigma_y)$	-0.65
		$1.36 - 0.081 \times 10^{-6} (\sigma_y^2 t)$	-0.69
		$1.38 - 0.013 (t)$	-0.71

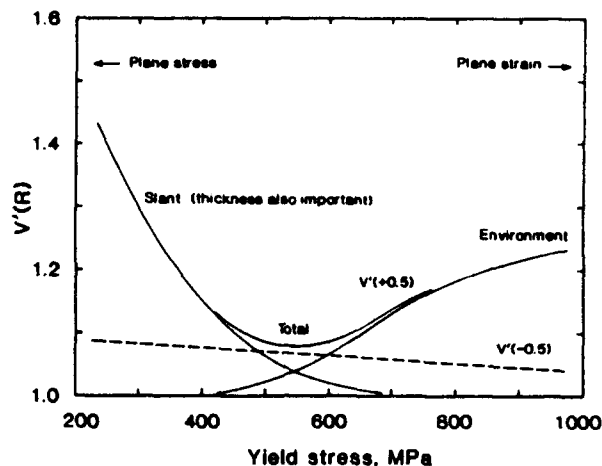


Fig. 8. Schematic diagram for the effect of yield strength and thickness on the crack growth rate correlation function $V'(R)$.

the growth rate increases much more for HY130 when the environment is changed to laboratory air than it does for Q1N (the same trend does not apply for the seawater environment).

The greater sensitivity of HY130 to moisture in the air could be expected to result in greater sensitivity to stress ratio at $R > 0$, where higher stress ratio opens the crack more and makes the crack tip more accessible to the environment.

Some results are not explained by this argument and are included here for completeness:

(a) On changing the environment from dry air to seawater, Q1N shows a larger increase in crack growth rate than HY130, but the sensitivity to R of the crack growth rate in HY130 in seawater is still higher than that of Q1N [9]. The values of $V'(0.5)$ for both Q1N and HY130 are similar in seawater, laboratory air and dry air.

(b) Cowling and Knott [11] observed strong dependence on R of the growth rate of semi-elliptical cracks in Q1N, in spite of weak environmental sensitivity (and plane strain conditions). This may be related to the fact that the cracks were short.

Figure 8 summarizes the present discussion in schematic form. For negative R , the correlation function $V'(R)$ decreases slightly with increasing yield stress but is not apparently affected by thickness. For positive R , there are two conflicting trends with increasing yield stress. For low yield strengths (and thicknesses) $V'(R)$ decreases with increasing yield stress (or thickness) as conditions of plane strain and flat fracture are approached. The change in $V'(R)$ can be attributed to a crack closure mechanism. For high yield strengths (and thicknesses) closure is not significant, but $V'(R)$ increases with yield strength because there is a concomitant increase in sensitivity to the testing environment. The correlation between yield strength and environmental sensitivity is unlikely to persist for steels whose compositions or microstructures differ widely from those of the quenched and tempered steels of the present study. Some of the scatter for the lower strength steels may be due to variations in their environmental sensitivity.

CONCLUSIONS

In this paper, measurements of the effect of stress ratio on the fatigue crack growth rate in quenched and tempered steels with a range of yield strengths have been reported. The results have

been compared with published measurements for other steels, aluminium alloys, austenitic stainless steel and a titanium alloy.

A crack growth rate correlation function $V'(R)$ has been derived which enables an experimental crack growth rate curve for $R = 0$ (or any available R) to be converted into a curve for any other R . The function $V'(R)$ is derived from da/dN versus ΔK curves, so it does not specifically relate to any particular mechanism.

This function reveals more clearly than previously proposed correlation functions (such as the crack closure function U) the effects of yield stress and thickness, because it reduces the amount of scatter.

The approach used here is to gradually refine the crack growth rate prediction. The major influence is of course the tensile part of ΔK . Of secondary importance is R . Further refinement is introduced by adjusting the R correction (i.e. the correlation function $V'(R)$) to take yield strength and thickness into account.

For steels, yield stress has a slight effect on crack growth rate for negative R . For positive R , the effect is greater but the growth rate becomes less sensitive to R as plane strain conditions are approached (with increasing strength or thickness), with the exception that higher strength quenched and tempered steels show increasing sensitivity to R . The latter trend is possibly due to increasing sensitivity to environment, but the evidence for this is not conclusive.

Aluminium alloys, austenitic stainless steel and titanium alloys have not been considered in the same detail, but show strong dependence of the crack growth rate on R . This is attributed to the conditions of plane stress under which most of these materials have been tested.

Acknowledgements—Most of the content of this paper was produced while the author was a visiting scientist at DRA Maritime Division, Dunfermline, U.K. The author thanks Mr I. Kilpatrick and other colleagues at DRA for their encouragement and support during this time. Thanks also to Dr J. Galsworthy of DRA, Holton Heath, for helpful discussion on environmental sensitivity.

REFERENCES

1. S. Chand and S. B. L. Garg (1985) Crack propagation under constant amplitude loading. *Engng Fract. Mech.* **21**, 1–30.
2. W. Elber (1971) The significance of fatigue crack closure. ASTM STP 486, ASTM, Philadelphia, pp. 230–242.
3. J. Schijve (1988) Fatigue crack closure: observations and technical significance. ASTM STP 982, ASTM, Philadelphia, pp. 5–34.
4. J. M. Finney and G. Deirmendjian (1992) Delta- K -effective: which formula? *Fatigue Fract. Engng Mater. Struct.* **15**, 151–158.
5. S. B. Singh and R. Kumar (1993) Experimental observations of fatigue crack growth in IS-1020 steel under constant amplitude loading. *Int. J. Press. Vessels Piping* **53**, 217–227.
6. M. Kurihara, A. Katoh and M. Kawahara (1986) Analysis on fatigue crack growth rates under a wide range of stress ratios. *Trans. ASME: J. Press. Vessel Tech.* **108**, 209–213.
7. E. D. Eason, J. D. Gilman, D. P. Jones and S. P. Andrew (1992) Technical basis for a revised fatigue crack growth rate reference curve for ferritic steels in air. *Trans. ASME: J. Press. Vessel Tech.* **114**, 80–86.
8. I. M. Robertson (1993) Measurement of the effects of stress ratio and changes of stress ratio on fatigue crack growth rate in a quenched and tempered steel. Accepted for publication in *Int. J. Fatigue*.
9. B. F. Jones (1984) The influence of environment and stress ratio on the low frequency fatigue crack growth behaviour of two medium-strength quenched and tempered steels. *Int. J. Fatigue* **6**, 75–81.
10. M. N. James and J. F. Knott (1985) An assessment of crack closure and the extent of the short crack regime in QIN (HY80) steel. *Fatigue Fract. Engng Mater. Struct.* **8**, 177–191.
11. J. M. Cowling and J. F. Knott (1989) Fatigue crack growth from small, semi-elliptic, hydrogen-induced cracks in QIN steel. *Fatigue Fract. Engng Mater. Struct.* **12**, 585–595.
12. A. Ohta, M. Kosuge and E. Sasaki (1978) Fatigue crack closure over the range of stress ratios from -1

- to 0.8 down to stress intensity threshold level in HT80 steel and SUS304 stainless steel. *Int. J. Fract.* **14**, 251-264.
13. S. Fukuda, S. Watari and K. Horikawa (1979) An experimental study of effect of welding residual stress upon fatigue crack propagation based on observation of crack opening and closure. *Trans. J. Weld. Res. Inst.* **8**, 105-111.
 14. F. K. Ibrahim (1989) Threshold stress intensity behaviour of cracked steel structural components. *Fatigue Fract. Engng Mater. Struct.* **12**, 543-552.
 15. Y. Z. Itoh, S. Suruga and H. Kashiwaya (1989) Prediction of fatigue crack growth rate in welding residual stress field. *Engng Fract. Mech.* **33**, 397-407.
 16. K. J. Kang, J. H. Song and Y. Y. Earmme (1989) Fatigue crack growth and closure through a tensile residual stress field under compressive loading. *Fatigue Fract. Engng Mater. Struct.* **12**, 363-376.
 17. H. R. Shercliff and N. A. Fleck (1990) Effect of specimen geometry on fatigue crack growth in plane strain-I. Constant amplitude response. *Fatigue Fract. Engng Mater. Struct.* **13**, 287-296.
 18. J. Woodtli, W. Muster and J. C. Radon (1986) Residual stress effects in fatigue crack growth. *Engng Fract. Mech.* **24**, 399-412.
 19. G. S. Booth and S. J. Maddox (1988) Correlation of fatigue crack growth data at different stress ratios. ASTM STP 982, ASTM, Philadelphia, pp. 516-527.
 20. A. J. McEvily (1988) On crack closure in fatigue crack growth. ASTM STP 982, ASTM, Philadelphia, pp. 35-43.
 21. D. Gan and J. Weertman (1981) Crack closure and crack propagation rates in 7050 aluminium. *Engng Fract. Mech.* **15**, 87-106.
 22. H. U. Stasi and J. D. Elen (1979) Crack closure and influence of cycle ratio R on fatigue crack growth in type 304 stainless steel at room temperature. *Engng Fract. Mech.* **11**, 275-283.
 23. R. J. Allen, G. S. Booth and T. Jutla (1988) A review of fatigue crack growth characterisation by linear elastic fracture mechanics. Part I—Principles and methods of data generation. *Fatigue Fract. Engng Mater. Struct.* **11**, 45-69.
 24. S. I. Kwun and M. E. Fine (1980) Fatigue macrocrack growth in tempered HY80, HY130 and 4140 steels: threshold and mid delta- K range. *Fatigue Engng Mater. Struct.* **3**, 367-382.

Accession For	
NTIS CRA&I	<input checked="" type="checkbox"/>
DTIC TAB	<input type="checkbox"/>
Unannounced	<input type="checkbox"/>
Justification	
By	
Distribution/	
Availability Codes	
Dist	Avail and/or Special
A-1	20